International Journal of Mass Spectrometry 283 (2009) 56–68

Contents lists available at ScienceDirect

International Journal of Mass Spectrometry

journal homepage: www.elsevier.com/locate/ijms

An experimental and theoretical study of alkali metal cation/methionine interactions

P.B. Armentrout*, Amy Gabriel, R.M. Moision[1]

Department of Chemistry, University of Utah, 315 S. 1400 E. Rm 2020, Salt Lake City, UT 84112, United States

ARTICLE INFO

Article history:
Received 28 October 2008
Received in revised form 16 January 2009
Accepted 20 January 2009
Available online 30 January 2009

In honor of our colleague and friend, Michael T. Bowers, on the occasion of his 70th birthday and in recognition of his many scientific contributions

Keywords:
Alkali metal cations
Amino acids
Bond energies
Collision-induced dissociation
Methionine

ABSTRACT

The interactions of alkali metal cations ($M^+ = Li^+$, Na^+, K^+) with the amino acid methionine (Met) are examined in detail. Experimentally, the bond energies are determined using threshold collision-induced dissociation of the M^+(Met) complexes with xenon in a guided ion beam mass spectrometer. Analyses of the energy dependent cross sections provide 0 K bond energies of 3.03 ± 0.13 eV, 2.09 ± 0.11 eV, and 1.47 ± 0.11 eV for complexes of Met with Li^+, Na^+, and K^+, respectively. All bond energy determinations include consideration of unimolecular decay rates, internal energy of reactant ions, and multiple ion-molecule collisions. Ab initio calculations at the MP2(full)/6-311 + G(2d,2p), B3LYP/6-311 + G(2d,2p), and B3P86/6-311 + G(2d,2p) levels with geometries and zero point energies calculated at the B3LYP/6-311G(d,p) level show good agreement with the experimental bond energies, especially for the sodium and potassium complexes. Ground state conformers are tridentate for Li^+ and Na^+, and subtle changes in the Met side-chain orientation are found to cause noticeable changes in the alkali metal binding energy. For K^+, tridentate and zwitterionic structures are nearly isoenergetic, with different levels of theory predicting different ground conformers. The combination of this series of experiments and calculations allows the influence of the functional groups of Met on the overall binding strength to be thoroughly explored.

© 2009 Elsevier B.V. All rights reserved.

1. Introduction

It is of fundamental interest to quantitatively investigate how the biologically important alkali metal cations interact with amino acids, and by extension how they interact with peptides and proteins. By studying such biologically relevant systems in the gas phase, intrinsic interactions can be quantitatively assessed in the absence of complicating solvent interactions. Such pairwise thermochemical information helps build a "thermodynamic vocabulary" [1] that can be used to enhance our understanding of complicated biological systems. In the present study, we extend previous work on the absolute binding energies of alkali metal cations with amino acids [2–8] to examine Li^+, Na^+, and K^+ binding with methionine (Met), one of the two common amino acids with sulfur in the side-chain ($R = -C_2H_4SCH_3$).

Interactions of metal ions with Met also have direct biological significance. For example, the interactions of alkali metal cations with methionine residues in the outer pore region of inwardly rectifying K^+ (Kir) ion channels have been implicated as a controlling feature for selective passage of different monocations [9]. Less direct evidence for the influence of alkali cations interacting with Met include the following observations. (i) Binding of potassium cations to S-adenosyl-L-methionine (AdoMet) synthetase, which catalyzes formation of AdoMet from ATP and L-methionine, maximizes the activity of this enzyme [10]. (ii) In turn, AdoMet has been shown to enhance Na^+/K^+ ATPase activity [11], whereas Met itself inhibits this activity [12].

The pairwise interactions of alkali metal cations with the 20 common amino acids have been studied extensively both experimentally and theoretically during the past decade [2–8,13–20]. For example, Cooks' kinetic method [21,22] has been used to measure the relative lithium cation binding affinities of most of the 20 common amino acids [13,14,19]. Similarly, sodium cation affinities for most of the 20 common amino acids, again probed using the kinetic method, have been determined by Bojesen et al. and Wesdemiotis and co-workers [13,18]. The average lithium cation binding free energy for Met at 373 K (determined using Gly and diethoxyethane as references) was reported by Feng et al. [19] as 211 ± 13 kJ/mol, which corresponds to a metal cation binding affinity (enthalpy) of about 266 kJ/mol at room temperature (calculated using ΔS_{373} and $(\Delta H_{373} - \Delta H_{298})$ values determined in the present study). For other amino acids, the values from Feng et al. have been found to be systematically low [4,5]. For sodium, Bojesen et al. [13] found that

* Corresponding author. Tel.: +1 801 581 7885; fax: +1 801 581 8433.
E-mail address: armentrout@chemistry.utah.edu (P.B. Armentrout).
[1] Present address: Department of Chemistry, UCSD, United States.

1387-3806/$ – see front matter © 2009 Elsevier B.V. All rights reserved.
doi:10.1016/j.ijms.2009.01.010

Met lay between Ser and Thr in their relative measurements of the sodium cation affinities of the amino acids. In the more quantitative study of Kish et al. [18], the sodium cation binding affinity for Met could not be determined because of an isobaric contaminant of the only heterodimer containing Met that could be produced. Methionine is not included among the experimental and theoretical potassium binding affinities compiled by Tsang and co-workers [23], but is found in the relative binding affinity determinations of the coinage metal cations, Cu^+ and Ag^+ [24,25].

These alkali metal cation amino acid complexes have also been studied theoretically [2–8,15,26–36], although we are unaware of any previous studies involving methionine. These calculations indicate that metal cations bind electrostatically to the functional groups of the amino acid backbone and side-chain. Such theoretical predictions have been confirmed by structural studies using infrared action spectra of sodiated Gly, proline (Pro) [20], and metallated tryptophan (Trp) [31], arginine (Arg) [32], serine (Ser) [33], threonine (Thr) [34], aspartic and glutamic acid (Asp, Glu) [35], in addition to thermodynamic studies involving threshold collision-induced dissociation (TCID) studies of various metalated α-amino acids [2–8,36].

The biological significance of these pairwise noncovalent interactions indicate that an examination of the metalated Met systems using a method that can provide absolute thermochemical measurements would be useful. In the present study, the binding affinities of Li^+, Na^+, and K^+ with Met are measured using TCID methods in a guided ion beam tandem mass spectrometer (GIBMS). Complementary quantum chemical calculations are performed for low-lying structures of these complexes and the free ligands at MP2(full), B3LYP, and B3P86 levels using a 6-311 + G(2d,2p) basic set with optimized structures and zero point energies determined at the B3LYP/6-311G(d,p) level. For the lithium complexes, calculations including core electron correlation on the lithium atom are also conducted to provide more accurate thermochemistry [37]. In addition to providing information necessary for interpretation of the experimental data as well as bond energies for comparison, such calculations allow an examination of how binding energies of the metal cation methionine complexes vary with conformation. As a number of low energy conformers exist for even simple amino acids, an understanding of the thermodynamic consequences of such conformational changes is useful in better understanding the thermodynamic implications in biological systems.

2. Experimental and computational section

2.1. General experimental procedures

The GIBMS used to measure the cross sections for TCID of the alkali metal cation Met complexes has been described previously in detail [38,39]. Briefly, the ions of interest are formed in a dc discharge flow tube (DC/FT) source. Alkali metal ions are generated at the cathode, a tantalum boat filled with the alkali metal located at the head of a 1-m long flow tube, by using a continuous dc discharge with typical operating conditions of 1.9–2.2 kV and 10–20 mA. The alkali metal cations are carried down the flow tube by a buffer gas (ca. 10% argon in helium) with normal operating pressures of 0.3–0.4 Torr. About 50 cm downstream from the discharge, the neutral ligand is introduced into the flow tube using a temperature controlled probe, which is heated to about 210 °C for Met. Complexes of interest are formed via three-body associative reactions of the alkali cation with Met in the flow of the He/Ar carrier gas. The complex ions are thermalized to 300 K (the temperature of the flow tube) both vibrationally and rotationally by undergoing ~10^5 collisions with the buffer gases as they drift along the 1 m long flow tube [3,4,40–45].

The ions are then extracted, focused, and accelerated through a magnetic momentum analyzer to select ions of interest. The mass-selected ions are decelerated and injected into a radio frequency (rf) octopole ion beam guide where ions are radially trapped [46]. The kinetic energy of the ions in the guide is controlled by the dc voltage applied to the octopole. The octopole passes through a gas cell of effective length 8.6 cm that contains the neutral reactant (Xe in the present experiments). All product and residual reactant ions drift to the end of the octopole where they are extracted and focused into a quadrupole mass filter for mass analysis. The ions are detected by a 27 kV conversion dynode-secondary electron scintillation detector [47] interfaced with fast pulse counting electronics. The raw ion intensities are converted to cross sections as described elsewhere [38]. The absolute cross sections are estimated to be accurate to ±20% with relative uncertainties of ±5%. Laboratory (lab) collision energies are converted to center-of-mass (CM) energies using the equation $E_{CM} = E_{lab}M/(M+m)$, where M and m are the reactant neutral and ion masses, respectively. All energies cited below are in the CM frame unless otherwise noted. The absolute energy scale and the corresponding full width at half-maximum (fwhm) of the ion beam kinetic energy distribution are determined by using the octopole as a retarding energy analyzer [38]. The energy spread is nearly Gaussian and has a typical fwhm of ~0.3 eV (lab).

It has been shown previously [48] that the pressure of the neutral reactant can influence the shape and onset of TCID cross sections because of the effects of multiple collisions. In order to obtain data free from pressure effects (i.e., at rigorously single collision conditions), data are collected at about 0.04 mTorr, 0.08 mTorr, and 0.15 mTorr, and the cross sections are extrapolated to zero reactant pressure prior to threshold analysis. A complete set of pressure measurements was reproduced at least three times for each system.

2.2. Threshold analysis

For endothermic reactions, the threshold energies can be extracted by fitting the energy dependent cross sections in the threshold region using Eq. (1),

$$\sigma(E) = \sigma_0 \sum \frac{g_i(E + E_i - E_0)^n}{E} \quad (1)$$

where σ_0 is an adjustable parameter that is energy independent, n is an adjustable parameter that describes the energy deposition efficiency during collision [39], E is the relative kinetic energy, and E_0 represents the CID threshold energy at 0 K. E_i are the internal energies of the rovibrational states i of the reactant ion with populations g_i, where $\Sigma g_i = 1$, such that $E + E_i$ is the total energy available to the colliding reactants. Vibrational frequencies and rotational constants used to calculate E_i and g_i are obtained from the calculations outlined in the next section. The Beyer–Swinehart–Stein–Rabinovitch algorithm [49–51] is used to evaluate the density of the rovibrational states and the relative populations g_i are calculated for a Maxwell–Boltzmann distribution at 300 K.

Because the metal–ligand complexes investigated here are relatively large, 10 heavy atoms for M^+(Met), the unimolecular dissociation kinetics must be included in the analysis of the CID cross sections. The time available for dissociation (τ) in the instrument used here is ~5×10^{-4} s (as previously measured by time-of-flight studies) [39]. If this is insufficient for the complex ions to dissociate, then products will not be observed until an energy higher than the true CID threshold, leading to a kinetic shift. These kinetic shifts are estimated by the incorporation of Rice–Ramsperger–Kassel–Marcus (RRKM) theory into Eq. (1), as described in detail elsewhere [52,53], which transforms

it into Eq. (2).

$$\sigma(E) = \left(\frac{n\sigma_0}{E}\right) \sum g_i \int_{E_0-E_i}^{E} (1 - e^{-k(E^*)\tau})(E - \varepsilon)^{n-1} d(\varepsilon) \quad (2)$$

Here ε is the energy transferred from translation into internal energy of the complex during the collision, E^* is the internal energy of the energized molecule (EM) after the collision, i.e., $E^* = \varepsilon + E_i$, with n, g_i, E_i, and E defined above. The term $k(E^*)$ is the unimolecular rate constant for dissociation of the EM as defined by RRKM theory [54–56] in Eq. (3),

$$k(E^*) = \frac{dN_{vr}^{\dagger}(E^* - E_0)}{h\rho_{vr}(E^*)} \quad (3)$$

where d is the reaction degeneracy, h is Planck's constant, $N_{vr}^{\dagger}(E^* - E_0)$ is the sum of rovibrational states of the transition state (TS) at an energy $E^* - E_0$, and $\rho_{vr}(E^*)$ is the density of rovibrational states of the EM at the available energy, E^*. In the limit that $k(E^*)$ is faster than the time-of-flight of the ions, the integration in Eq. (2) recovers Eq. (1).

To evaluate the rate constants in Eq. (3), vibrational frequencies and rotational constants for the EM and all TSs are required. Because the metal–ligand interactions in the complexes studied here are mainly long-range electrostatic interactions (ion-dipole, ion-quadrupole, and ion-induced dipole interactions), the most appropriate model for the TS is generally a loose association of the ion and neutral ligand fragments [2,3,43,57–59], even for multidentate ligands [60–63]. Therefore, the TSs are treated as product-like, such that the TS frequencies are those of the dissociated products. The transitional frequencies are treated as rotors, a treatment that corresponds to a phase space limit (PSL), as described in detail elsewhere [52,53]. For M^+L complexes dissociating to $M^+ + L$, the three transitional mode rotors have rotational constants equal to those of the ligand product. The 2D external rotations are treated adiabatically but with centrifugal effects included [64]. In the present work, the adiabatic 2-D rotational energy is treated using a statistical distribution with an explicit summation over all possible values of the rotational quantum number [52].

Before comparing with the experimental data, the calculated cross section is convoluted over the kinetic energy distribution of the ion beam and thermal energy distribution of the neutral collision gas (Doppler broadening), as described elsewhere [38]. A nonlinear least-squares analysis is used to provide optimized values for σ_0, E_0, and n. The uncertainty associated with E_0 is estimated from the range of threshold values determined from different data sets with variations of vibrational frequencies (±10% for most vibrations and a factor of two for the $M^+ - L$ modes) and the parameter n, variations in τ by a factor of 2, and the uncertainty in the absolute energy scale, 0.05 eV (lab).

In deriving the final optimized bond energies at 0 K, two assumptions are made. First, there is no activation barrier in excess of the endothermicity for the loss of ligands, which is generally true for ion–molecule reactions, especially the heterolytic noncovalent bond cleavages considered here [65]. Second, the measured threshold is assumed to correspond to dissociation of the ground state reactant to ground state ion and neutral ligand products. Given the relatively long experimental time frame available ($\sim 5 \times 10^{-4}$ s) for the energized complexes to explore phase space, we assume that the dissociating products are able to rearrange to their ground state conformations upon dissociation. The appropriateness of this assumption for the Met ligand is nicely verified by the good agreement between our experimental results with theoretical values, see below.

2.3. Computational details

A simulated annealing procedure [2] using the AMBER forcefield [66] was used to search for possible stable structures in each system's conformational space. All possible structures identified in this way were further optimized using NWChem [67] at the HF/3-21G level [68,69]. Unique structures for each system within about 50 kJ/mol of the lowest energy structure (about 50 for each complex) were further optimized using Gaussian 03 [70] at the B3LYP/6-31G(d) level [71–73] with the "loose" keyword (maximum step size of 0.01 au and an RMS force of 0.0017 au) to facilitate rapid convergence. The 10–15 lowest energy structures obtained from this procedure were then chosen for higher-level geometry optimizations and frequency calculations using density functional theory (DFT) at the B3LYP/6-311G(d,p) level [74,75]. This level of theory has been shown to be adequate for accurate structural descriptions of comparable metal cation–ligand systems [2–8]. Zero-point vibrational energy (ZPE) corrections were determined using these vibrational frequencies after scaling by 0.9804 [76]. Single point energy calculations were carried out for the lowest 7–11 optimized structures at the B3LYP, B3P86, and MP2(full) levels using the 6-311 + G(2d,2p) basis set. Basis set superposition errors (BSSE) in all bond dissociation energy calculations were estimated using the full counterpoise (cp) method [77,78]. Previous work [2,3,59,79,80] has indicated that BSSE corrections on alkali metal systems are generally small for DFT calculations and we find this to be true here as well. Both B3LYP and B3P86 calculations have BSSE corrections of 0.8 – 3.4 kJ/mol, whereas the MP2(full) values have BSSE corrections of 7 – 14 kJ/mol.

A comprehensive analysis of lithium cation affinities reveals that core electron correlation on the lithium cation is needed to better describe the interaction energy of lithium with a variety of ligands [37]. Therefore, we also optimized the ground state structures of Li^+(Met) systems at the MP2(full) level of theory using the cc-pCVDZ basis set for Li^+ and cc-pVDZ basis set for other atoms, designated as cc-pVDZ(Li-C) below. Single point energies were calculated using B3LYP, B3P86, and MP2(full) levels with the cc-pCVTZ for Li^+ and aug-cc-pVTZ basis sets for other atoms, designated as aug-cc-pVTZ(Li-C) below. No counterpoise corrections are made to these single point energies as these have been shown to reduce the accuracy of the MP2 computational results [37]. We also checked whether geometries calculated using aug-cc-PVDZ(Li-C) altered these results, but found that bond lengths were the same within 0.01 Å, bond angles within 1°, and bond energies within 1 kJ/mol.

3. Results

3.1. Cross sections for collision-induced dissociation

Experimental cross sections were obtained for the interaction of Xe with M^+(Met), where $M^+ = Li^+$, Na^+ and K^+, as a function of collision energy. Fig. 1 shows representative data extrapolated to zero pressure of Xe for collision-induced dissociation (CID) of these complexes. Over the energy ranges examined, the loss of the intact amino acid, reaction (4), is seen in all three M^+(Met) systems.

$$M^+(Met) + Xe \rightarrow M^+ + Met + Xe \quad (4)$$

The magnitudes of the cross sections increase from Li^+ to Na^+ to K^+, reflecting the decrease in the apparent threshold for dissociation. This is consistent with previous threshold CID bond dissociation energy measurements of metallized amino acids [1–3,8] and many other ligands [81]. In no system was a ligand exchange process forming an ion containing Xe observed, however, the lithium sys-

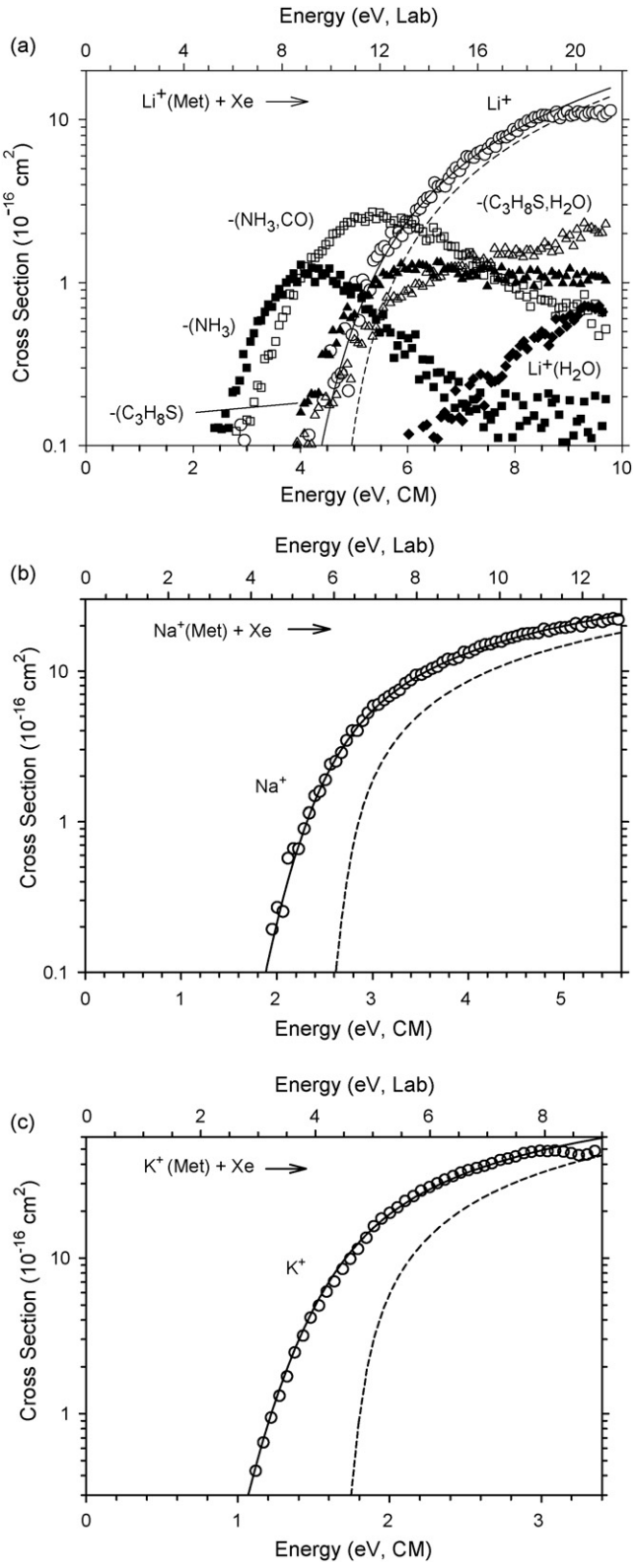

Fig. 1. Zero pressure extrapolated cross sections for collision-induced dissociation of Li^+(Met), Na^+(Met), and K^+(Met) with xenon as a function of kinetic energy in the center-of-mass frame (lower *x*-axis) and the laboratory frame (upper *x*-axis). Solid lines show the best fit to the data using the model of Eq. (2) convoluted over the neutral and ion kinetic and internal energy distributions. Dashed lines show the model cross sections in the absence of experimental kinetic broadening for reactions with an internal energy of 0 K.

tem exhibits several alternate decomposition channels, reactions (5)–(9).

$$Li^+(Met) + Xe \rightarrow Li^+(C_5H_8O_2S) + NH_3 + Xe \quad (5)$$

$$\rightarrow Li^+(C_4H_8OS) + NH_3 + CO + Xe \quad (6)$$

$$\rightarrow Li^+(C_2H_3O_2N) + C_2H_5SCH_3 + Xe \quad (7)$$

$$\rightarrow Li^+(C_2HON) + C_2H_5SCH_3 + H_2O + Xe \quad (8)$$

$$\rightarrow Li^+(H_2O) + [C_5H_9ONS] + Xe \quad (9)$$

Loss of ammonia in reaction (5) is the lowest energy decomposition pathway for protonated methionine [82]. The energy dependence of these cross sections clearly shows that ammonia is lost first in reaction (5), followed by CO in this system. Reaction (7) is loss of the side-chain, where the ionic product can then subsequently lose water in reaction (8), again consistent with the energy dependence exhibited. The high energy process (9) could conceivably compete with reaction (8), such that the lithium ion retains the water product rather than the larger more strongly bound organic fragment.

3.2. Threshold analysis and results

Methionine losses in reactions (4) were modeled using Eq. (2). Fig. 1 shows that the experimental cross sections are reproduced well by Eq. (2) over extended energy and magnitude ranges. The optimized parameters of Eq. (2) for all systems using molecular parameters for the ground state complexes and PSL transition states calculated at the B3LYP/6-311 + G(d) level (see next section) are reported in Table 1, including threshold values with and without RRKM lifetime analysis. The difference between these values equal the kinetic shifts for M^+(Met), 1.31, 0.46, and 0.27 eV for Li^+, Na^+, and K^+, respectively. These are 0.2–0.3 eV higher than for the analogous complexes of Thr [5], which has a shorter side-chain. Thus, the size of the kinetic shift varies such that higher E_0 values and more complicated ligands yield larger kinetic shifts. The relatively large kinetic shift values found here indicate the importance of incorporating RRKM theory into the threshold analysis when dealing with such complex systems. These threshold values have been published previously as preliminary results [1].

Fig. 1a clearly indicates that competition between the loss of the intact amino acid, reaction (4), and the other fragmentation reactions (5)–(9) is possible in the Li^+(Met) system. Despite the lower energies of some of these alternate decomposition reactions, reaction (4) is the dominant reaction at high energies, indicating that this process is entropically favored. This is also indicated by the observation that the energy dependences of the other cross sections are influenced once reaction (4) becomes accessible. In order to estimate the effect of competition with these fragmentation reactions on the threshold for reaction (4), we modeled our data by explicitly including the competitive channels as a sum of the cross sections for reactions (5)–(9). This should be reasonable as NH_3 loss in reaction (5) and the subsequent decomposition of this product ion in reaction (6) dominate the alternate product spectrum. Therefore the details of this competitive analysis are analogous to those for Li^+(Ser) and Li^+(Thr) [85], where water loss dominated the alternate products. In this study, a detailed theoretical exploration of the pathways for the various alternate decomposition pathways was conducted, but such a complicated elucidation is beyond the scope of the present work. Therefore, the tight transition state needed here to characterize ammonia loss was estimated by examining the difference in molecular parameters between the TS found for loss of water from Li^+(Ser) and the ground state Li^+(Ser) complex, which has a similar tridentate structure to Li^+(Met). This comparison shows that the high frequencies are essentially unchanged in the two molecules, there is a missing frequency (the reaction coordinate) at about 1700 cm^{-1}, and frequencies below ~1600 cm^{-1} are

Table 1
Fitting parameters of Eq. (2), threshold dissociation energies at 0 K, and entropies of activation at 1000 K for CID of M^+ (Met) with Xe[a].

Reactant	Ionic product	σ_0	n	E_0 (eV)[b]	E_0 (PSL) (eV)	$\Delta S^\dagger_{1000}$ (J/mol K)
Li^+(Met)	Li^+	45.1 (6.1)	1.9 (0.2)	4.64 (0.19)	3.33 (0.13)	73 (6)
Li^+(Met)[c]	Li^+	29.7 (8.4)	1.0 (0.1)	–	3.03 (0.13)	76 (6)
	Li^+(Met–NH_3)	12.5 (3.5)	1.0 (0.1)	–	2.05 (0.10)	7 (4)
Na^+(Met)	Na^+	23.5 (2.1)	1.4 (0.1)	2.55 (0.06)	2.09 (0.11)	53 (13)
K^+(Met)	K^+	74.5 (3.5)	1.3 (0.1)	1.74 (0.07)	1.47 (0.11)	50 (12)

[a] Uncertainties are listed in parentheses.
[b] Does not include lifetime effects.
[c] Competitive fitting results for cross sections of Li^+ and the sum of all other product channels, see text for details.

uniformly smaller by about 5% in the TS. Thus, molecular parameters of the tight TS needed here can be estimated by starting with vibrations from the Li^+(Met) ground state complex, removing a frequency of ~1700 cm^{-1} as the reaction coordinate, and scaling the frequencies below 1600 cm^{-1} by 0.95. The molecular parameters of the tight TS used to analyze the ammonia loss channel here were chosen in this fashion. It was found that the data could be accurately reproduced using such molecular parameters as shown in Fig. 2. Variations in the frequency scaling applied, 0.95 ± 0.02, are included in the uncertainties deduced for this modeling, but significantly, the data could not be reproduced with fidelity if the frequencies <1600 cm^{-1} of the tight TS were scaled by either 0.90 or 1.00. The recommended final results for this competitive fit are provided in Table 1.

As for the Li^+(Ser) and Li^+(Thr) systems, competitive modeling lowers the threshold for Li^+ production by ~0.3 eV (Table 1), which correctly reflects the expected effect of competition on the higher energy Li^+ channel. In addition, the n value is close to unity for the competitive analysis, smaller than the single channel modeling results. As demonstrated previously, the parameter n characterizes the energy deposition efficiency upon collision [39], with a smaller number indicating better energy transfer efficiency and a value near unity corresponding to the line-of-centers model. Conservatively, the BDE obtained using single channel fitting should be viewed as an upper limit and the competitive modeling result is treated as the best value from the present experiments. As discussed below, the competitive modeling value is in much better agreement with various trends in the bond energies for different metal cations and amino acids.

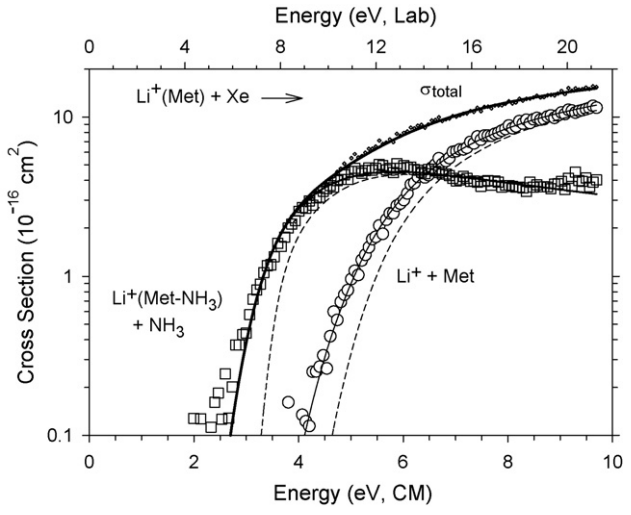

Fig. 2. Competitive analysis of the cross sections for Li^+ and the composite dissociation channel for Li^+(Met), see text. Solid lines show the model cross sections convoluted over the neutral and ion kinetic and internal energies. Dashed lines show the model cross sections in the absence of experimental energy broadening for reactants with an internal energy of 0 K.

Table 1 also includes $\Delta S^\dagger_{1000}$ values, which reflect the looseness of the transition states. In all cases, the $\Delta S^\dagger$ values for losing intact ligands are 50–75 J/(mol K), which is consistent with the assumption of loose transition states for the M^+(Met) systems. In contrast, the $\Delta S^\dagger$ value for the ammonia loss channel from Li^+(Met) is much lower, properly reflecting its tighter character.

3.3. Theory: methionine and M^+(Met)

As described above, seven to eleven of the lowest energy structures of neutral Met and its metallated complexes were optimized at the B3LYP/6-311G(d,p) level of theory. Single point energies including zero point energy (ZPE) corrections are calculated at three different levels of theory, relative to the lowest energy conformer, and are given in Tables 2 and 3. For neutral amino acids, there are three main types of structures with different intramolecular hydrogen bonding that are indicated by Nx (where x refers to the backbone hydrogen bonding motif). The N1 conformers have NH···OC and OH···OC hydrogen bonds, whereas N2 has a OH···N hydrogen bond. The other possible conformer, N3, has NH···OH and OH···OC hydrogen bonds where the former is much less stable than the NH···OC structure. For Met, these designations are augmented with the orientation of the $-C_2H_4SCH_3$ side-chain including both the CCCS and CCSC dihedral angles (designated as either g = gauche for angles between 50° and 135° and t = trans for angles >135°), Table 2. The six lowest-lying conformations of Met are shown in Fig. 3 with some structural information provided in Table 2. For the purposes of the data analysis, it is most important to find that these low lying structures are within a couple of kJ/mol of one another at all three levels of theory.

For the M^+(Met) complexes, low-lying and representative higher energy conformations are shown in Fig. 4. Table 3 lists the relative energies calculated here with additional geometric parameters detailed in Table 4. We use the nomenclature established previously for M^+(Gly) [2,3,86,87], where the notation in brackets describes the metal binding sites for each conformer and the letters after the dash indicate the dihedral angles of ∠HOCO, ∠CCCC, ∠CCCS, and ∠CCSC, respectively (where c = cis indicates angles <50°). In con-

Table 2
Theoretical structural parameters and relative energies of neutral methionine[a].

Structure[b]	∠CCCS (°)	∠CCSC (°)	Relative energies (kJ/mol)		
			B3LYP	B3P86	MP2(full)
N1-tg	176.5	−77.1	**0.0**	0.4	0.3
N1-gt	−72.4	167.7	0.6	0.3	**0.0**
N1-tt	177.0	−175.6	0.7	1.3	2.1
N2-tg	176.3	69.2	3.0	0.2	4.6
N2-gt	−60.0	−179.9	3.5	**0.0**	2.5
N2-g_+g	68.6	76.5	5.6	1.7	4.3
N2-g–g	−62.7	113.4	6.4	0.5	0.8

[a] Structures are geometry optimized and have zero point energy corrections calculated at the B3LYP/6-311G(d,p) level. Final relative values are taken from single point energies at the levels indicated using a 6-311 + G(2d,2p) basis set. Ground states in bold.

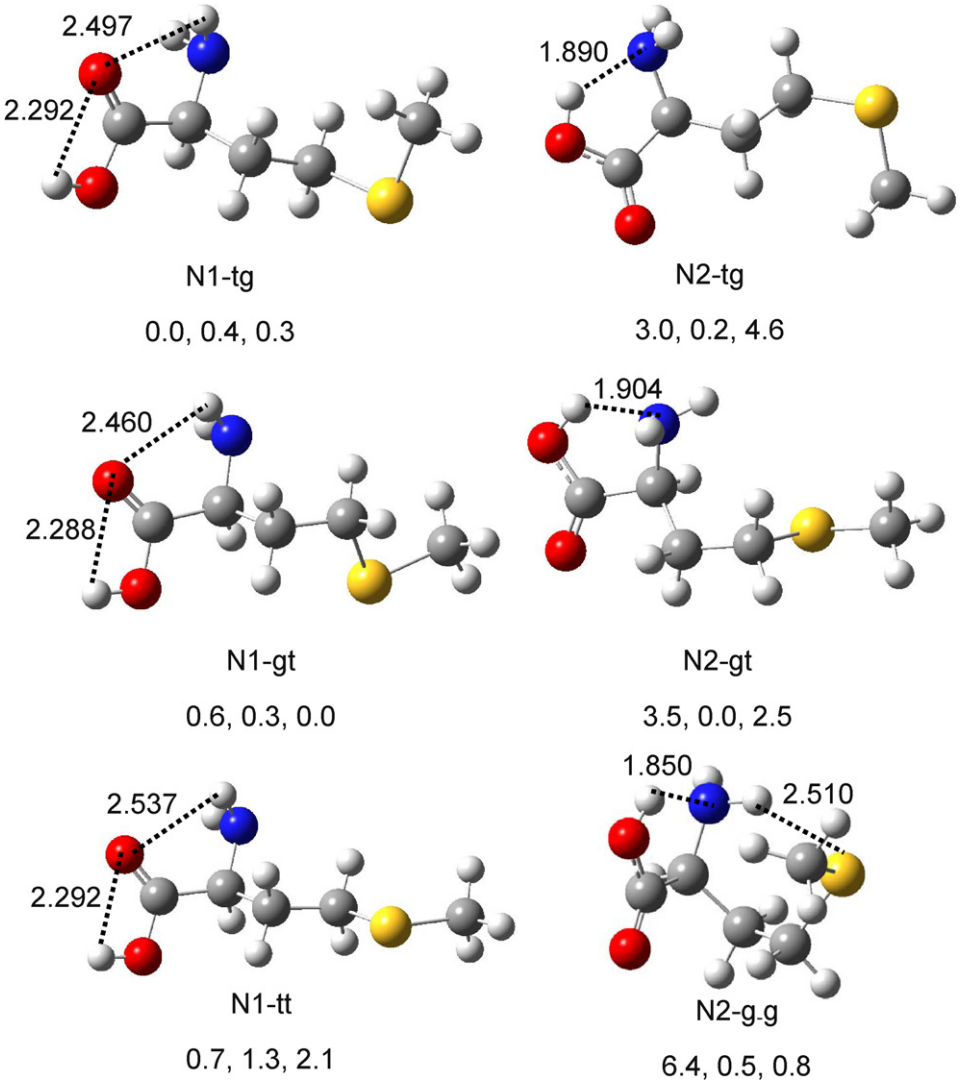

Fig. 3. Methionine low energy structures calculated at the B3LYP/6-311G(d,p) level. Numbers show energies relative to the ground state structure calculated at the B3LYP, B3P86, and MP2(full) levels using a 6-311 + G(2d,2p) basis set corrected for zero point energies. Dashes indicate hydrogen bonds with lengths shown in Å.

trast to these previous works, we no longer utilize the arbitrary numbering designation of M*y* (where *y* refers to a specific structure as first introduced by Jensen for M^+(Gly) complexes [26]).

At all levels of theory, the lowest energy structure for Li^+(Met) and Na^+(Met) is the [N,CO,S]-ccgt conformer, a tridentate structure in which the metal ion binds to the backbone amino nitrogen, backbone carboxyl oxygen, and the side-chain sulfur. For K^+(Met), this structure is the ground state at the MP2(full) level of theory and is 3 or 8 kJ/mol above the ground state at the two DFT levels of theory. As shown in Table 3, the [N,CO,S]-ccgt conformer is the lowest energy structure by at least 5 kJ/mol and 6 kJ/mol for Li^+ and Na^+, respectively, with the very similar [N,CO,S]-ccgg conformers being next in energy. Overall, the four tridentate [N,CO,S] structures lie within 13 kJ/mol, 12 kJ/mol, and 9 kJ/mol of one another for the Li^+, Na^+, and K^+ systems, respectively. It is interesting that such variations in the side-chain orientation lead to changes in the binding energetics. An examination of the geometric parameters in Table 4 (as well as several others not compiled here) did not locate any particular coordinate that correlates uniformly with relative energy. The M–OC, M–N, and M–S bond lengths do not vary appreciably with conformation and neither do ∠MCS(CH_3) dihedral angles that quantify the orientation of the metal with the sulfur group. For the [N,CO,S] structures, conformations with a trans ∠CCSC dihedral angle (ccgt and cggt) are uniformly lower in energy than the analogues that have a gauche orientation (ccgg and cggg, respectively). Overall, the energetic variations appear to be cumulative effects associated with metal cation ligand bond lengths coupled with strained dihedral angles imposed by the multidentate ligand solvation of the cation. Thus, the variations in energy with conformation are larger for the smaller, higher charge density metal cations.

The next lowest energy type of structure for Li^+(Met) and Na^+(Met) and the DFT ground state for K^+(Met) is the zwitterionic [CO_2^-] in which the metal cation interacts with the carboxylate anion and the sulfur side-chain hydrogen bonds to the NH_3^+ group (Fig. 4). There are three conformations, tggg, ttgg, and tggt, which all lie within 5 kJ/mol of one another for all three metal cations. In contrast to the [N,CO,S] conformers, [CO_2^-] structures with a trans ∠CCSC dihedral angle (tggt) are higher in energy than the analogues that have a gauche orientation (tggg). For K^+(Met), the relative energies of the [CO_2^-]-tggg and [N,CO,S]-ccgt conformers vary over a 9 kJ/mol range depending on the level of theory, with B3P86 strongly and B3LYP weakly preferring the zwitterion, whereas MP2(full) weakly prefers the tridentate charge solvated structure. At much higher energies, there is another zwitterionic structure, [CO_2^-,S], where the metal cation binds both the carboxylate anion and the side-chain sulfur. Again there are three [CO_2^-,S]

conformations, tggt, tg$_-$gg, and tg$_+$gg, which are similar in energy. For Li^+, Na^+, and K^+ complexes, these conformations are calculated to lie 14–25 kJ/mol, 20–32 kJ/mol, and 24–31 kJ/mol, respectively, above the analogous [CO_2^-] conformers.

For Li^+(Met), a series of bidentate [N,CO] structures are found to lie 31–52 kJ/mol above the ground state (GS) conformer. These same structures lie 21–35 kJ/mol above the GS for Na^+(Met) and 14–29 kJ/mol above the K^+(Met) GS conformer. For K^+(Met), tridentate [COOH,S] structures in which the metal cation binds to both oxygens of the carboxylic acid as well as the side-chain sulfur are relatively low-lying. These conformations lie 7–16 kJ/mol above the GS, whereas they are much higher in energy for Na^+(Met), 23–30 kJ/mol. In Li^+(Met), these conformations are still higher in energy (37–54 kJ/mol) and, in two of the variations, collapse to a bidentate [CO,S] structure in which the lithium cation no longer coordinates with the hydroxyl group. The relative stability of the [COOH] coordination for K^+ compared to the smaller alkali cations is a general result for most amino acids [2,3,8,31–34]. Notably, the K^+(Met)[CO_2^-,S] zwitterionic analogues of the [COOH,S] conformations are found to lie 14–18 kJ/mol higher in energy, which contrasts with the [CO_2^-] and [COOH] conformations where the charge solvated structure lies higher in energy by 15–19 kJ/mol. Clearly the zwitterionic structure is strongly favored by the intramolecular solvation of the NH_3^+ group by the sulfur side-chain. Similar trends are also found for the Li^+(Met) and Na^+(Met) complexes and eventually reach the point where the Li^+(Met)[COOH] structures collapse to the zwitterionic [CO_2^-] structure at this level of theory.

3.4. Conversion from 0 K to 298 K and excited conformers

Conversion from 0 K bond energies to 298 K bond enthalpies and free energies is accomplished using the rigid rotor/harmonic oscillator approximation with rotational constants and vibrational frequencies calculated at the B3LYP/6-311G(d,p) level. These ΔH_{298} and ΔG_{298} values along with the conversion factors and 0 K enthalpies measured here are reported in Table 5. The uncertainties listed are determined by scaling most of the vibrational frequencies by ±10% along with two-fold variations in the metal–ligand frequencies. Because there is some ambiguity as to the ground state structure for the free Met ligand (Table 2), conversion factors for N1-tg, N1-gt, and N2-gt were all considered. Values for the two N1 conformers are essentially identical but the $\Delta H_{298} - \Delta H_0$ values

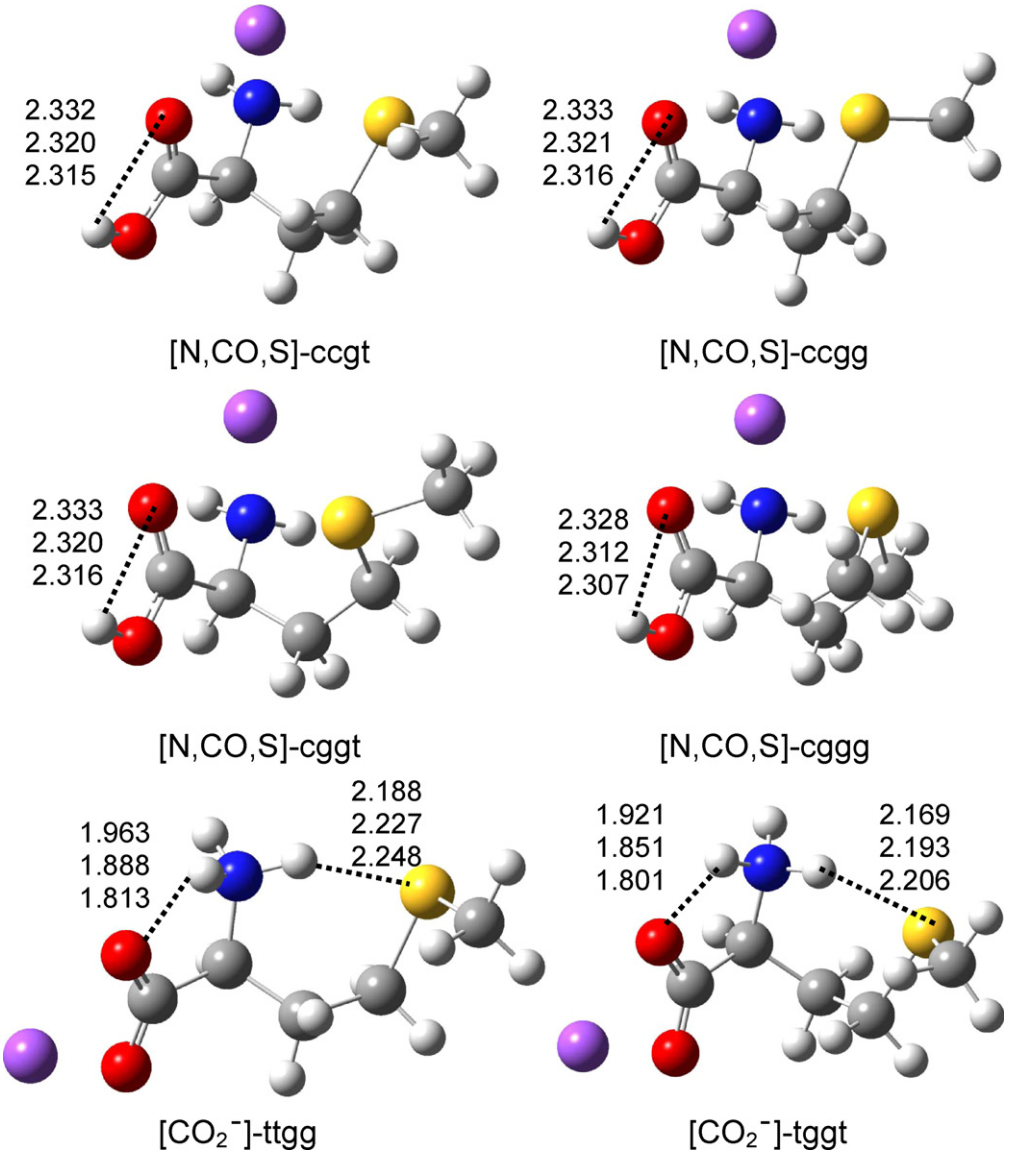

Fig. 4. Na^+(Met) low energy structures calculated at the B3LYP/6-311G(d,p) level. Dashes indicate hydrogen bonds with lengths shown in Å for Li^+(Met) (top), Na^+(Met), and K^+(Met) (bottom). The [CO,S]-tcgg structure shown (next page) is for Li^+(Met).

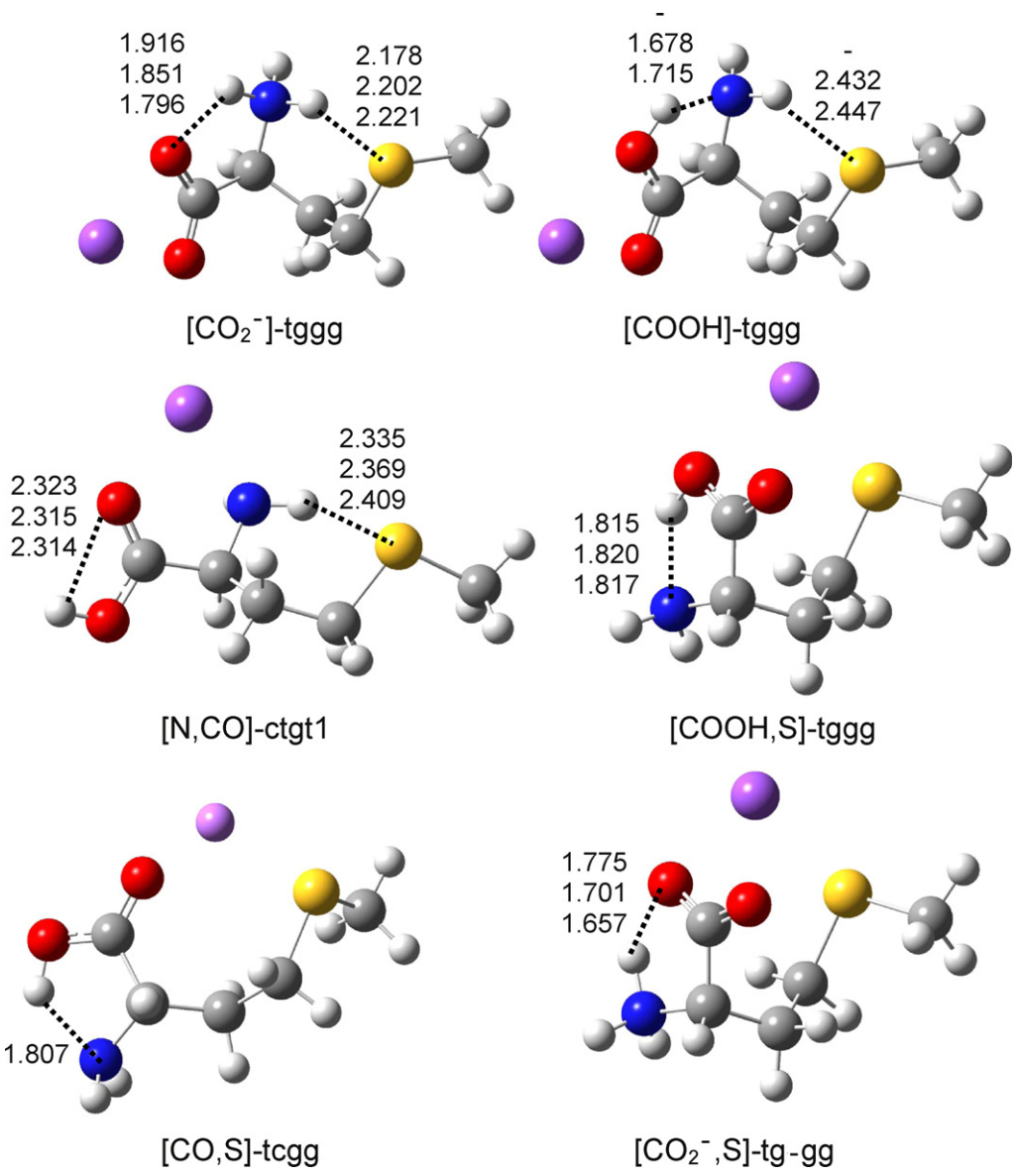

Fig. 4. (*Continued*).

for the N2 conformer are about 1.0 kJ/mol lower than those shown in Table 5 and the $T\Delta S_{298}$ values are about 2.5 kJ/mol lower. These differences operate in opposite directions on the final ΔG_{298} values, such that differences associated with different conformations of the Met product are less than 2 kJ/mol, well within the uncertainties listed.

We also calculated the relative ΔG_{298} values for the four to eight lowest energy structures. In general, the relative ΔG_{298} excitation energies are comparable to the analogous differences in the ΔH_0 values (Table 3) although the free energies of the [N,CO,S]-cggg conformers drop by about 2 kJ/mol and the [CO_2^-]-tggt conformers increase by about 2 kJ/mol relative to the other conformers. Using the ΔG_{298} values to calculate an equilibrium population of conformers shows that the calculated ground state structures for M^+(Met) system should be dominant in the room temperature ion source. Excited conformers are calculated to comprise 9–13% of the total for Li^+(Met) with the [N,CO,S]-ccgg conformer accounting for 7–11%. For Na^+(Met), excited conformers comprise 9–22% with alternate [N,CO,S] conformers contributing 8–14% and [CO_2^-] conformers adding 1–13%. For K^+(Met), the results depend drastically on the level of theory. For DFT results, the [CO_2^-]-tggg conformer comprises 41–56% of the calculated population, with [CO_2^-]-ttgg adding 32%, [N,CO,S]-ccgt contributing 3–16%, [CO_2^-]-tggt adding 7–8%, and the other three [N,CO,S] conformers contributing less than 1.5% each. At the MP2(full) level, these relative populations are calculated as 20, 4, 40, and 6%, with [N,CO,S]-cggg, cggt, and ccgg contributing another 24, 4, and 2%, respectively. To investigate the effect of having a different conformer populating the K^+(Met) cations generated in the flow tube ion source, we analyzed the data using the molecular parameters of several of the low energy conformers. The threshold energies change by less than 1 kJ/mol and this effect is included in the uncertainties listed in the tables.

4. Discussion

4.1. Comparison of theoretical and experimental bond dissociation energies

The theoretical BDEs for the M^+(Met) complexes, where $M^+ = Li^+$, Na^+, and K^+, calculated at three levels of theory for all metal cations with and without the core correlation basis set for Li^+ are compared to the experimental values in Table 6. We find that all three

Table 3
Relative Energies (kJ/mol) of Low-lying Conformers of M^+(Met)[a].

Name	Structure	B3LYP	B3P86	MP2(full)
Li^+(Met)	[N,CO,S] ccgt	0.0	0.0	0.0
	ccgg	6.1	6.3	5.2
		6.8[b]	*6.7*[b]	*4.8*[b]
	cggt	11.4	12.0	11.7
	cggg	12.8	12.8	12.0
	[CO_2^-] ttgg	27.0	23.4	32.7
	tggg	27.4	23.1	30.2
	tggt	29.7	25.8	34.0
	[N,CO] ctgt1	32.9	31.0	38.1
	cgg$_-$t	34.2	34.0	40.6
	ctgt2	37.6	37.6	46.0
	[CO,S] tcgg	37.8	37.4	53.7
	tggt	39.9	37.6	50.7
	[N,CO] cgg$_+$t	40.5	39.3	52.1
	[CO_2^-,S] tg$_-$gg	51.9	48.3	46.9
	[COOH,S] tggg	52.4	47.9	50.7
	[CO_2^-,S] tggt	53.0	49.8	49.0
	tg$_+$gg	55.5	52.6	50.5
	[COOH]	[c]	[c]	[c]
Na^+(Met)	[N,CO,S] ccgt	0.0	0.0	0.0
	ccgg	7.3	6.7	6.6
	cggt	8.8	8.7	8.2
	[CO_2^-] tggg	9.9	3.5	9.9
	ttgg	10.2	4.6	13.2
	[N,CO,S] cggg	12.3	10.5	8.7
	[CO_2^-] tggt	12.8	6.7	14.5
	[N,CO] ctgt1	23.4	21.1	27.2
	cgg$_-$t	26.9	24.8	29.0
	[COOH,S] tggg	28.3	23.0	23.8
	tggt	28.6	23.4	25.5
	tcgg	29.9	24.6	25.8
	[N,CO] ctgt2	31.4	27.3	34.5
	[N,CO] cgg$_+$t	33.0	29.6	30.2
	[COOH] tggg	37.6	29.8	38.4
	ttgg	37.7	30.2	40.8
	[CO_2^-,S] tg$_-$gg	37.7	32.3	32.4
	tggt	38.2	33.2	34.0
	tg$_+$gg	40.0	35.2	34.4
	[COOH] tggt	40.6	33.2	43.0
K^+(Met)	[CO_2^-] tggg	0.0	0.0	1.3
	ttgg	0.3	1.1	4.9
	tggt	2.4	2.8	2.4
	[N,CO,S] ccgt	2.7	7.7	0.0
	cggt	9.3	14.4	5.5
	ccgg	9.7	15.2	6.9
	cggg	10.9	14.8	3.2
	[COOH,S] tggt	12.7	14.8	9.7
	tcgg	13.6	15.8	8.1
	tggg	13.7	14.8	7.1
	[N,CO] ctgt1	14.4	19.3	15.3
	[COOH] ttgg	15.2	16.1	19.8
	tggg	15.3	15.9	17.2
	tggt	18.1	19.2	21.8
	[N,CO] ctgt2	20.7	25.2	25.1
	cgg$_+$t	25.2	28.8	22.3
	[CO_2^-,S] tggt	28.5	29.6	26.0
	tg$_-$gg	28.8	29.8	24.0
	tg$_+$gg	29.9	31.2	25.4

[a] All values calculated at the level of theory indicated using the 6-311 + G(2d,2p) basis set with geometries and zero point energies calculated at the B3LYP/6-311G(d,p) level of theory.

[b] Values calculated at the level of theory indicated using the aug-cc-pVTZ(Li-C) basis set with geometries and ZPEs calculated at the MP2(full)/cc-pVDZ(Li-C) level.

[c] All conformers collapse to [CO_2^-].

theoretical methods (B3LYP, B3P86, and MP2) yield BDE values for M^+(Met) that differ little from one another. Fig. 5 shows that the theoretical values are in good agreement with our experimental values especially with regard to the trends. Mean absolute deviations (MADs) range from 1 kJ/mol to 7 kJ/mol (Table 6). When the geometry optimizations and single point energy calculations of the Li^+(Met) systems include core correlation on lithium, the

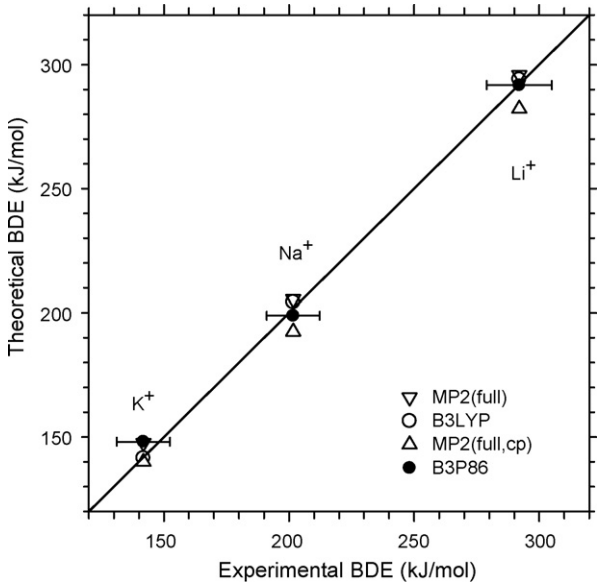

Fig. 5. Experimental versus theoretical 0 K bond dissociation energies (in eV) calculated at the MP2(full)/6-311 + G(2d,2p)//B3LYP/6-311G(d,p) with (triangle) and without (inverted triangle) counterpoise corrections, B3LYP/6-311 + G(2d,2p)//B3LYP/6-311G(d,p) (open circles), and B3P86/6-311 + G(2d,2p)//B3LYP/6-311G(d,p) (closed circles) levels of theory. The diagonal line indicates perfect agreement.

corresponding theoretical BDEs increase (mainly because counterpoise corrections are not included) but the MADs change very little (Table 6). Overall, all three levels of theory give comparable agreement with the experimental values, although the B3LYP values agree best, with the MP2(full) and MP2(full,cp) values bracketing the experimental results.

4.2. Comparison to literature bond energies

Feng et al. [19] measured the binding free energies (ΔG) for dissociation of Li^+(Met) using the kinetic method with glycine (Gly) and diethoxyethane (DEE) as reference bases. They report an average value of 211 ± 13 kJ/mol at an ion temperature of 373 K. (This temperature is used because the reference values used correspond to this temperature, whereas the estimated temperature in the ion trap was 325 ± 30 K.) A corresponding 0 K enthalpy value of 260 ± 13 kJ/mol is included in Table 6, as deduced here by using ΔS_{373} = 147 J mol^{-1} K^{-1} and ($\Delta H_{373} - \Delta H_0$) = 6 ± 1 kJ/mol calculated here at the B3LYP/6-311G(d,p) level of theory. This enthalpy is much lower than our experimental and theoretical results, as also recently found for the lithium ion affinities of proline, serine, and threonine [4,5]. There, a number of possible contributions to these discrepancies were discussed, such as a revision in the values used to anchor the absolute values. This would raise the value of Feng et al. by 8 ± 4 kJ/mol, but this still lies 24 kJ/mol below our experimental and theoretical results. Although the absolute values from Feng et al. do not appear reliable, their relative measurements place the lithium ion affinity of Met above that of Thr by 2 kJ/mol (albeit with a relative uncertainty of 6 kJ/mol). This relative affinity agrees with our independent measurements, which also place the lithium ion affinity of Met, $D_0(Li^+–Met)$ = 292 ± 12 kJ/mol, above that of Thr, $D_0(Li^+–Thr)$ = 285 ± 13 kJ/mol [5]. Here the relative uncertainty in our measurements is somewhat smaller than the absolute uncertainties given because various systematic errors in the measurements cancel. We estimate that the relative uncertainty in our measurements is comparable to that of the kinetic method studies, i.e., about 6 kJ/mol. (Note that if the Met bond energy is not corrected for competition, the value obtained here would be 321 ± 12 kJ/mol, such that the difference with the Thr bond energy

Table 4
B3LYP/6-311G(d,p) geometric parameters of M^+(Met) structures[a].

Structure	r(M^+–OC) (Å)			r(M^+–N) (Å)			r(M^+–S) (Å)		
	Li	Na	K	Li	Na	K	Li	Na	K
[N,CO,S] ccgt	1.934	2.284	2.619	2.064	2.451	2.865	2.438	2.801	3.217
	1.964			*2.067*			*2.458*		
ccgg	1.937	2.289	2.622	2.049	2.434	2.839	2.450	2.809	3.241
	1.968			*2.055*			*2.463*		
cggt	1.922	2.271	2.600	2.084	2.472	2.905	2.463	2.825	3.250
cggg	1.919	2.265	2.598	2.078	2.467	2.913	2.448	2.840	3.263
[CO_2^-] ttgg	1.913	2.255	2.604	1.955[b]	2.290[b]	2.658[b]			
tggg	1.924	2.277	2.619	1.945[b]	2.302[b]	2.645[b]			
tggt	1.919	2.273	2.605	1.947[b]	2.304[b]	2.656[b]			
[N,CO] ctgt1	1.865	2.242	2.596	2.019	2.403	2.819			
cgg$_-$t	1.862	2.232	[c]	2.012	2.399	[c]			
ctgt2	1.862	2.230	2.581	2.017	2.400	2.825			
cgg$_+$t	1.846	2.212	2.551	2.031	2.419	2.849			
[CO_2^-,S] tg$_-$gg	1.961	2.296	2.619	1.980[b]	2.321[b]	2.668[b]	2.577	3.055	3.527
tggt	1.948	2.285	2.593	2.003[b]	2.349[b]	2.694[b]	2.579	3.107	3.526
tg$_+$gg	1.947	2.285	2.594	2.007[b]	2.350[b]	2.709[b]	2.581	3.035	3.520
[COOH,S] tcgg	1.761[d]	2.282	2.618		2.560[e]	2.910[e]	2.392[d]	2.902	3.355
tggt	1.775[d]	2.293	2.606		2.509[e]	2.880[e]	2.426[d]	2.907	3.402
tggg	1.930	2.310	2.641	2.206[e]	2.456[e]	2.801[e]	2.500	2.920	3.421
[COOH] ttgg	[f]	2.278	2.614	[f]	2.418[e]	2.841[e]			
tggg	[f]	2.287	2.634	[f]	2.400[e]	2.796[e]			
tggt	[f]	2.286	2.626	[f]	2.399[e]	2.809[e]			

Structure	∠CCCC (°)			∠CCCS (°)			∠CCSC (°)		
	Li	Na	K	Li	Na	K	Li	Na	K
[N,CO,S] ccgt	−45.6	−50.2	−52.3	−63.3	−67.5	−67.7	−179.0	−167.6	−158.6
	−45.3			*−65.0*			*180.0*		
ccgg	−39.9	−40.8	−44.2	−59.2	−65.4	−67.3	−68.7	−66.7	−60.2
	−39.4			*−61.2*			*−63.7*		
cggt	−90.5	−85.7	−82.8	59.2	61.6	62.9	179.8	167.9	158.2
cggg	−95.2	−87.2	−81.3	54.8	56.2	58.8	66.5	64.0	68.2
[CO_2^-] ttgg	175.6	177.0	177.5	68.7	69.8	71.0	78.1	77.4	77.2
tggg	−56.4	−56.1	−55.2	−65.2	−65.9	−66.2	−78.0	−78.2	−78.4
tggt	−60.3	−61.1	−60.7	−73.3	−75.0	−74.9	158.2	160.1	159.4
[N,CO] ctgt1	176.5	173.9	173.3	82.2	81.5	81.2	176.5	−171.4	−174.5
cgg$_-$t	−60.8	−58.5	[c]	−73.2	−70.9	[c]	172.1	173.1	[c]
ctgt2	158.0	157.7	159.4	62.6	63.9	65.7	179.8	179.1	177.2
cgg$_+$t	−84.5	−85.5	−85.1	51.2	50.5	52.0	−176.0	−176.4	−178.9
[CO_2^-,S] tg$_-$gg	−51.8	−54.0	−57.5	76.0	77.9	78.6	62.5	64.3	71.0
tggt	−48.9	−51.3	−56.4	83.4	85.0	81.7	175.7	169.8	169.7
tg$_+$gg	48.5	50.0	49.9	−82.3	−85.5	−87.1	−70.8	−77.0	−82.5
[COOH,S] tcgg	83.9[d]	46.8	47.9	−97.8[d]	−85.9	−88.1	−68.3[d]	−72.5	−78.7
tggt	−53.3[d]	−58.7	−64.5	115.0[d]	87.5	81.6	−178.4[d]	174.4	175.4
tggg	−58.7	−60.5	−62.5	80.3	82.3	82.1	68.1	68.9	73.1
[COOH] ttgg	[f]	174.2	173.7	[f]	75.8	76.3	[f]	81.0	80.3
tggg	[f]	−58.3	−57.4	[f]	−66.0	−65.3	[f]	−77.1	−77.2
tggt	[f]	−65.9	−66.0	[f]	−75.9	−75.9	[f]	174.6	175.7

[a] Values in italics calculated at the MP2(full)/cc-pVDZ(Li-C) level.
[b] r(M^+–O) (Å).
[c] Collapses to [N,CO,S].
[d] [CO,S].
[e] r(M^+–OH) (Å).
[f] Collapses to [CO_2^-].

Table 5
Enthalpies and Free Energies of M^+(Met) Binding at 0 and 298 K in kJ/mol[a].

Complex	ΔH_0[b]	$\Delta H_{298}-\Delta H_0$[c]	ΔH_{298}	$T\Delta S_{298}$[c]	ΔG_{298}
Li^+(Met)	292.0 (12.2)	5.8 (1.2)	297.8 (12.2)	43.5 (4.6)	254.3 (13.1)
Na^+(Met)	201.7 (10.6)	3.2 (1.2)	204.9 (10.7)	40.5 (4.9)	164.4 (11.5)
K^+(Met)	141.8 (10.6)	2.0 (1.0)	143.8 (10.7)	37.0 (5.0)	106.8 (12.1)

[a] Uncertainties are listed in parentheses.
[b] Experimental values from this work (Table 1). Competitive fitting value for Li^+(Met).
[c] Values were computed using standard formulas and molecular constants calculated at the B3LYP/6-311+G(d,p) level and correspond to the N1 conformer of Met and the [N,CO,S]-ccgt conformer of M^+(Met). The uncertainties correspond to 10% variations in the vibrational frequencies of the ligands and two-fold variations in the metal ligand-frequencies.

Table 6
Experimental and theoretical binding energies (kJ/mol) at 0 K for M^+(Met)[a].

Complex	Experiment		Theory[b]			
	This work	Literature	B3LYP (cp)	B3P86 (cp)	MP2(full)	MP2 (full, cp)
Li^+(Met)	292.0 (12.2)	260 (13)[c]	294.1 *297.8*[d]	291.7 *292.4*[d]	295.8 *296.2*[d]	282.2
Na^+(Met)	201.7 (10.6)		204.3	198.9	205.5	192.5
K^+(Met)	141.8 (10.6)		141.5	148.1	147.6	141.1
MAD			1.7 (1.2) *2.9*(*2.8*)	3.1 (3.0) *3.2*(*3.0*)	4.5 (1.2) *4.6*(*1.1*)	6.6 (5.1)

[a] Uncertainties are listed in parentheses.
[b] All structures geometry optimized and have zero point energy corrections calculated at the B3LYP/6-311G(d,p) level. Final energies are taken from single point energies calculated at the levels indicated using 6-311 + G(2d,2p) basis set including counterpoise (cp) corrections, except as noted.
[c] Value from Feng et al. [19], adjusted to ΔH_0 as described in text.
[d] Values in italics have geometries optimized and zero point energies calculated at the MP2(full)/cc-pVDZ(Li-C) level with single point energies calculated at the levels indicated using the aug-cc-pVTZ(Li-C) basis set without cp corrections.

would be much greater than that implied by the kinetic method experiments.)

Kish et al. [18] were unable to measure the sodium cation binding affinity of methionine along with the other amino acids because of an isobaric contaminant in the only complex with Met they could form under their source conditions, one with serine. The latter observation suggests that the sodium cation binding affinity of Met is near that of Ser. Likewise, Bojesen et al. [13] found that Met lay between Ser and Thr in their relative measurements of the sodium cation affinities of the amino acids. Previously, we have measured $D_0(Na^+–Ser)$ as 200 ± 8 kJ/mol and $D_0(Na^+–Thr)$ as 204 ± 10 kJ/mol [5], such that the present value of $D_0(Na^+–Met)$ = 202 ± 11 kJ/mol does indeed fall nicely between these two systems.

4.3. Side-chain substituent effect

Metal cations interact with amino acids by electrostatic ion induced-dipole and ion–dipole forces that lead to solvation of the charge by coordination of the functional groups of the amino acids. Our results for the BDEs required to remove the alkali metal cation from M^+(Met), where $M^+ = Li^+$, Na^+, and K^+ (Table 6), decrease from Li^+ to K^+ because the electrostatic interactions decrease with the increasing bond distances necessitated by the increasing size of the metal cation (0.70 Å, 0.98 Å, and 1.33 Å, respectively [88]). As the metal changes from Li^+ to Na^+, the BDEs to Met drop approximately 90 kJ/mol (~31%), and then by another 60 kJ/mol (~30%) from Na^+ to K^+. The relative BDE decreases are comparable to those measured in our laboratory for M^+(Gly), M^+(Pro), M^+(Ser), and M^+(Thr), 26–33% for Li^+ to Na^+ and 23–27% for Na^+ to K^+ [2–4,37,89]. When the M^+(Met) BDEs are compared to those of metalated aliphatic amino acids, such as M^+(Gly), as well as other bidentate amino acids such as M^+(Pro), they are larger in part because the side-chain sulfur group participates in the bonding. Compared to the M^+(Gly) systems, the binding energies of M^+(Met) are increased by ~72 kJ/mol (~33%) for Li^+, ~38 kJ/mol (~23%) for Na^+, and ~21 kJ/mol (~17%) for K^+. Because Li^+ has a much higher charge density than Na^+ and K^+, there is a larger enhancement when changing from bidentate to tridentate binding. Likewise for Na^+ versus K^+ where the difference is less pronounced. These enhancements are similar to those for Ser and Thr where the hydroxyl side-chains also contribute to the binding: ~61 kJ/mol and 65 kJ/mol (~30%) for Li^+, 36 kJ/mol and 40 kJ/mol (~20%) for Na^+, and 24 kJ/mol and 28 kJ/mol (~20%) for K^+. (Note that in all of these comparisons, if the bond energy of Li^+(Met) is uncorrected for competition, the enhancement found is anomalously large.)

Rodgers and Armentrout have previously noted that there is a simple linear dependence of the BDEs for both Na^+ and K^+ on the polarizability of the Gly (6.6 Å^3), Pro (10.3 Å^3), Met (14.6 Å^3), Phe (18.1 Å^3), Tyr (18.8 Å^3), and Trp (22.0 Å^3) amino acids, as shown in Fig. 6 [1,8]. (These isotropic molecular polarizabilities were calculated at the PBE0/6-311 + G(2d,2p) level of theory using the B3LYP/6-311G(d,p) optimized geometries in the metallated complexes. This level of theory has been shown to provide polarizabilities that are in good agreement with measured values [90]. Values for free ligands are within 2% of the values for the frozen structures from the metallated complexes for all the three metal cations.) This clearly indicates the importance of ion-induced dipole interactions on the quantitative bond strengths. In contrast, Na^+ and K^+ BDEs to Ser (8.6 Å^3), Thr (10.5 Å^3), Asp (10.45 Å^3), Asn (11.2 Å^3), Glu (12.2 Å^3), and Gln (13.0 Å^3) do not fall on the same correlation line, but lie above it. Interestingly, the values for Ser, Thr, Asn, and Gln basically fall on lines parallel with those for Gly, Pro, Met, Phe, Tyr, and Trp, whereas the values for Asp and Glu are intermediate. In our work on the acidic amino acids and their amide derivatives [6,7], the ground state structures of the metallated complexes are found to be tridentate bound to the backbone carbonyl, backbone amino group, and the side-chain carbonyl. We noted that the acidic amino acids were bound less tightly than the amide derivatives (by 14 ± 1 kJ/mol for Na^+ complexes and 9 ± 1 kJ/mol for K^+ complexes) because the hydroxyl group is electron withdrawing in contrast to the amide group. Given this observation, it seems likely that the difference between the correlation lines can be attributed to the local dipole moment of the side-chain coordinating site. Met, Phe,

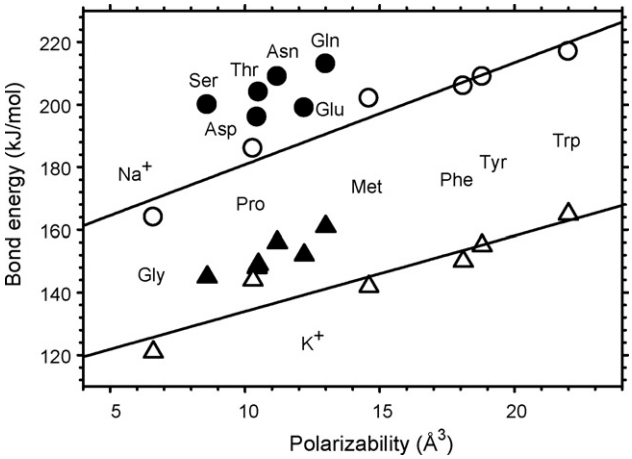

Fig. 6. Absolute sodium (circles) and potassium (triangles) cation bond energies to amino acids as a function of polarizability of the amino acid. Values for Gly [2,3], Pro [4], Met (Table 6), Phe, Tyr, and Trp [8] are shown by open symbols and used to determine the correlation lines shown. Values for Ser, Thr [5], Asp, Glu, Asn, and Gln [6,7] are shown by closed symbols.

Tyr, and Trp have small side-chain dipoles, whereas Ser, Thr, Asn, and Gln have larger ones, with Asp and Glu intermediate. This conclusion is also consistent with a comparison of the structures of M^+(Ser/Thr) and M^+(Met). In the GS complexes of Ser and Thr, which have virtually identical structures with one another, theory finds that the metal ion prefers to lie in the HOC plane (∠MCOH dihedral angles of 179–175° for Li^+–K^+), i.e., aligned with the dipole moment of the hydroxyl group [5]. In contrast, the metal ions in the GS Met complexes have ∠MCS(CH_3) dihedral angles of 118–128° for Li^+–K^+, indicating that the metal ions interact with one of the two sp^3-like lone pair orbitals on sulfur, thereby mediating the interaction of the metal cation with the local dipole. Notably, this alignment is achieved in Ser and Thr even though its side-chain is shorter and thus less flexible than that in Met.

5. Conclusion

The kinetic energy dependences of the collision-induced dissociation (CID) of M^+(Met), where $M^+ = Li^+$, Na^+, and K^+, are examined in a guided ion beam mass spectrometer. The primary cross section in all cases is the loss of amino acid from the complex, although extensive fragmentation by other routes is also found for Li^+(Met). The apparent threshold for removing Met follows the order of Li^+(Met) > Na^+(Met) > K^+(Met), as expected for the variations in charge density on the metal ion. BDEs at 0 K for losing Met from the complexes (Table 6) are obtained by detailed modeling of the experimental cross sections, including competition with the alternate low-energy decomposition pathways found for Li^+(Met).

Three different levels of quantum chemical calculations including zero point energy corrections and counterpoise corrections for basis set superposition errors were performed for all M^+(Met) complexes, as well as calculations employing basis sets with core correlation on Li (cc-pCVTZ) and aug-cc-pVTZ for other atoms of Li^+(Met). The calculated BDEs for losing Met from the M^+(Met) complexes agree well with our experimental values (Table 6).

The experimental 0 K BDEs of M^+(Met) are larger than those of aliphatic amino acids, Gly and Pro, but less than those of aromatic amino acids (Phe, Tyr, and Trp). These observations suggest that the metal cation is chelated to the sulfur functional group in the side-chain of Met, generally in agreement with theory, forming a tridentate binding pattern similar to the aromatic amino acid cases [8]. The aromatic amino acids have larger polarizabilities than Met, such that they interact more strongly with the metal cation. Comparison with other metallated amino acids (Ser, Thr, Asp, Glu, Asn, and Gln) that are also tridentate finds that Met has comparable binding affinities even though it has a larger polarizability. This is attributed to differences in the local dipole moments of the various side-chain functionalities.

Acknowledgments

This work is supported by the National Science Foundation, CHE-0748790. A grant of computer time from the Center for High Performance Computing at the University of Utah is gratefully acknowledged. AG thanks the University of Utah REU Program for support and Drs. R.M. Moision and C. Iceman for their assistance. Thanks also to a reviewer for reminding us of the importance of zwitterionic structures.

References

[1] M.T. Rodgers, P.B. Armentrout, Acc. Chem. Res. 37 (2004) 989.
[2] R.M. Moision, P.B. Armentrout, J. Phys. Chem. A 106 (2002) 10350.
[3] R.M. Moision, P.B. Armentrout, Phys. Chem. Chem. Phys. 6 (2004) 2588.
[4] R.M. Moision, P.B. Armentrout, J. Phys. Chem. A 110 (2006) 3933.
[5] S.J. Ye, A.A. Clark, P.B. Armentrout, J. Phys. Chem. B 112 (2008) 10291.
[6] A.L. Heaton, R.M. Moision, P.B. Armentrout, J. Phys. Chem. A 112 (2008) 3319.
[7] A.L. Heaton, P.B. Armentrout, J. Phys. Chem. B 112 (2008) 12056.
[8] C. Ruan, M.T. Rodgers, J. Am. Chem. Soc. 126 (2004) 14600.
[9] E. Wischmeyer, F. Doring, A. Karschin, FEBS Lett. 466 (2000) 115.
[10] M.S. McQueney, G.D. Markham, J. Biol. Chem. 270 (1995) 18277.
[11] M.D. Brown, P.K. Dudeja, T.A. Brasitus, Biochem. J. 251 (1988) 215.
[12] F.M. Stefanello, F. Chiarani, A.G. Kurek, C.M.D. Wannmacher, M. Wajner, A.T.S. Wyse, Int. J. Dev. Neurosci. 23 (2005) 651.
[13] G. Bojesen, T. Breindahl, U.N. Andersen, Org. Mass Spectrom. 28 (1993) 1448.
[14] U.N. Andersen, G. Bojesen, J. Chem. Soc. Perkins Trans. 2 (1997) 323.
[15] S. Hoyau, K. Norrman, T.B. McMahon, G. Ohanessian, J. Am. Chem. Soc. 121 (1999) 8864.
[16] B.A. Cerda, C. Wesdemiotis, Analyst 125 (2000) 657.
[17] V. Ryzhov, R.C. Dunbar, B.A. Cerda, C. Wesdemiotis, J. Am. Soc Mass Spectrom. 11 (2000) 1037.
[18] M.M. Kish, G. Ohanessian, C. Wesdemiotis, Int. J. Mass Spectrom. 227 (2003) 509.
[19] W.Y. Feng, S. Gronert, C.B. Lebrilla, J. Phys. Chem. A 107 (2003) 405.
[20] C. Kapota, J. Lemaire, P. Maitre, G. Ohanessian, J. Am. Chem. Soc. 126 (2004) 1836.
[21] R.G. Cooks, P.H. Wong, Acc. Chem. Res. 31 (1998) 379.
[22] R.G. Cooks, J.T. Koskinen, P.D. Thomas, J. Mass Spectrom. 34 (1999) 85.
[23] J.K.-C. Lau, C.H.S. Wong, P.S. Ng, F.M. Siu, N.L. Ma, C.W. Tsang, Chem. Eur. J. 9 (2003) 3383.
[24] B.A. Cerda, C. Wesdemiotis, J. Am. Chem. Soc. 117 (1995) 9734.
[25] V.W.-M. Lee, L. Hongbo, T.-C. Lau, R. Guevremont, K.W.M. Siu, J. Am. Soc. Mass Spectrom. 9 (1998) 760.
[26] F. Jensen, J. Am. Chem. Soc. 114 (1992) 9533.
[27] S. Hoyau, G. Ohanessian, Chem. Eur. J. 4 (1998) 1561.
[28] T. Marino, N. Russo, M. Toscano, Inorg. Chem. 40 (2001) 6439.
[29] T. Marino, N. Russo, M. Toscano, J. Phys. Chem. B 107 (2003) 2588.
[30] T. Marino, N. Russo, M. Toscano, J. Inorg. Biochem. 79 (2000) 179.
[31] N.C. Polfer, J. Oomens, R.C. Dunbar, Phys. Chem. Chem. Phys. 8 (2006) 2744.
[32] M.W. Forbes, M.F. Bush, N.C. Polfer, J. Oomens, R.C. Dunbar, E.R. Williams, R.A. Jockusch, J. Phys. Chem. A 111 (2007) 11759.
[33] P.B. Armentrout, M.T. Rodgers, J. Oomens, J.D. Steill, J. Phys. Chem. A 112 (2008) 2248.
[34] M.T. Rodgers, P.B. Armentrout, J. Oomens, J.D. Steill, J. Phys. Chem. A 112 (2008) 2258.
[35] J.T. O'Brien, J.S. Prell, J.D. Steill, J. Oomens, E.R. Williams, J. Phys. Chem. A 112 (2008) 10823.
[36] J.S. Klassen, S.G. Anderson, A.T. Blades, P. Kebarle, J. Phys. Chem. 100 (1996) 14218.
[37] M.T. Rodgers, P.B. Armentrout, Int. J. Mass Spectrom. 267 (2007) 167.
[38] K.M. Ervin, P.B. Armentrout, J. Chem. Phys. 83 (1985) 166.
[39] F. Muntean, P.B. Armentrout, J. Chem. Phys. 115 (2001) 1213.
[40] R.H. Schultz, K.C. Crellin, P.B. Armentrout, J. Am. Chem. Soc. 113 (1991) 8590.
[41] E.R. Fisher, P.B. Armentrout, J. Chem. Phys. 94 (1991) 1150.
[42] E.R. Fisher, B.L. Kickel, P.B. Armentrout, J. Chem. Phys. 97 (1992) 4859.
[43] M.T. Rodgers, P.B. Armentrout, J. Phys. Chem. A 101 (1997) 1238.
[44] M.T. Rodgers, P.B. Armentrout, Int. J. Mass Spectrom. 185/186/187 (1999) 359.
[45] M.T. Rodgers, P.B. Armentrout, J. Phys. Chem. A 103 (1999) 4955.
[46] D. Gerlich, Adv. Chem. Phys. 82 (1992) 1.
[47] N.R. Daly, Rev. Sci. Instrum. 31 (1960) 264.
[48] D.A. Hales, L. Lian, P.B. Armentrout, Int. J. Mass Spectrom. Ion Processes. 102 (1990) 269.
[49] T.S. Beyer, D.F. Swinehart, Commun. Assoc. Comput. Mach. 16 (1973) 379.
[50] S.E. Stein, B.S. Rabinovich, J. Chem. Phys. 58 (1973) 2438.
[51] S.E. Stein, B.S. Rabinovich, Chem. Phys. Lett. 49 (1977) 183.
[52] M.T. Rodgers, K.M. Ervin, P.B. Armentrout, J. Chem. Phys. 106 (1997) 4499.
[53] M.T. Rodgers, P.B. Armentrout, J. Chem. Phys. 109 (1998) 1787.
[54] R.G. Gilbert, S.C. Smith, Theory of Unimolecular and Recombination Reactions, Blackwell Scientific, London, 1990.
[55] D.G. Truhlar, B.C. Garrett, S.J. Klippenstein, J. Phys. Chem. 100 (1996) 12771.
[56] K.A. Holbrook, M.J. Pilling, S.H. Robertson, Unimolecular Reactions, Wiley, New York, 1996.
[57] F. Meyer, F.A. Khan, P.B. Armentrout, J. Am. Chem. Soc. 117 (1995) 9740.
[58] H. Koizumi, P.B. Armentrout, J. Am. Soc. Mass Spectrom. 12 (2001) 480.
[59] S.J. Ye, R.M. Moision, P.B. Armentrout, Int. J. Mass Spectrom. 253 (2006) 288.
[60] M.B. More, D. Ray, P.B. Armentrout, J. Phys. Chem. A 101 (1997) 831.
[61] M.B. More, D. Ray, P.B. Armentrout, J. Phys. Chem. A 101 (1997) 4254.
[62] M.B. More, D. Ray, P.B. Armentrout, J. Phys. Chem. A 101 (1997) 7007.
[63] S.J. Ye, P.B. Armentrout, J. Phys. Chem. A 112 (2008) 3587.
[64] E.V. Waage, B.S. Rabinovitch, Chem. Rev. 70 (1970) 377.
[65] P.B. Armentrout, J. Simons, J. Am. Chem. Soc. 114 (1992) 8627.
[66] D.A. Pearlman, D.A. Case, J.W. Caldwell, W.R. Ross, T.E. Cheatham, S. DeBolt, D. Ferguson, G. Seibel, P. Kollman, Comput. Phys. Commun. 91 (1995) 1.
[67] E.J. Bylaska, W.A. de Jong, K. Kowalski, T.P. Straatsma, M. Valiev, D. Wang, E. Aprà, T.L. Windus, S. Hirata, M.T. Hackler, Y. Zhao, P.-D. Fan, R.J. Harrison, M. Dupuis, D.M.A. Smith, J. Nieplocha, V. Tipparaju, M. Krishnan, A.A. Auer, M. Nooijen, E. Brown, G. Cisneros, G.I. Fann, H. Früchtl, J. Garza, K. Hirao, R. Kendall, J.A. Nichols, K. Tsemekhman, K. Wolinski, J. Anchell, D. Bernholdt, P. Borowski, T. Clark, D. Clerc, H. Dachsel, M. Deegan, K. Dyall, D. Elwood, E. Glendening, M. Gutowski, A. Hess, J. Jaffe, B. Johnson, J. Ju, R. Kobayashi, R. Kutteh, Z. Lin, R. Littlefield, X. Long, B. Meng, T. Nakajima, S. Niu, L. Pollack, M. Rosing, G. Sandrone, M. Stave, H. Taylor, G. Thomas, J.V. Lenthe, A. Wong, Z. Zhang, NWChem,

A Computational Chemistry Package for Parallel Computers, Pacific Northwest National Laboratory, Richland, Washington 99352, 2003.
[68] C.C. Roothaan, Rev. Mod. Phys. 23 (1951) 69.
[69] J.S. Binkley, J.A. Pople, W.J. Hehre, J. Am. Chem. Soc. 102 (1980) 939.
[70] M.J. Frisch, G.W. Trucks, H.B. Schlegel, G.E. Scuseria, M.A. Robb, J.R. Cheeseman, J.A. Montgomery, T. Vreven, K.N. Kudin, J.C. Burant, J.M. Millam, S.S. Iyengar, J. Tomasi, V. Barone, B. Mennucci, M. Cossi, G. Scalmani, N. Rega, G.A. Petersson, H. Nakatsuji, M. Hada, M. Ehara, K. Toyota, R. Fukuda, J. Hasegawa, M. Ishida, T. Nakajima, Y. Honda, O. Kitao, H. Nakai, M. Klene, X. Li, J.E. Knox, H.P. Hratchian, J.B. Cross, C. Adamo, J. Jaramillo, R. Gomperts, R.E. Stratmann, O. Yazyev, A.J. Austin, R. Cammi, C. Pomelli, J.W. Ochterski, P.Y. Ayala, K. Morokuma, G.A. Voth, P. Salvador, J.J. Dannenberg, V.G. Zakrzewski, S. Dapprich, A.D. Daniels, M.C. Strain, O. Farkas, D.K. Malick, A.D. Rabuck, K. Raghavachari, J.B. Foresman, J.V. Ortiz, Q. Cui, A.G. Baboul, S. Clifford, J. Cioslowski, B.B. Stefanov, G. Liu, A. Liashenko, P. Piskorz, I. Komaromi, R.L. Martin, D.J. Fox, T. Keith, M.A. Al-Laham, C.Y. Peng, A. Nanayakkara, M. Challacombe, P.M.W. Gill, B. Johnson, W. Chen, M.W. Wong, C. Gonzalez, J.A. Pople, Gaussian 03, Revision B. 02, Gaussian, Inc., Pittsburgh, PA, 2003.
[71] A.D. Becke, J. Chem. Phys. 98 (1993) 5648.
[72] C. Lee, W. Yang, R.G. Parr, Phys. Rev. B 37 (1988) 785.
[73] G.A. Petersson, T. Tensfeldt, J.A. Montgomery, J. Chem. Phys. 94 (1991) 6091.
[74] A.D. McLean, G.S. Chandler, J. Chem. Phys. 72 (1980) 5639.
[75] R. Krishnan, J.S. Binkley, R. Seeger, J.A. Pople, J. Phys. Chem. 72 (1980) 650.
[76] J.B. Foresman, A.E. Frisch, Exploring Chemistry with Electronic Structure Methods, Gaussian, Inc., Pittsburgh, PA, 1996.
[77] S.F. Boys, R. Bernardi, Mol. Phys. 19 (1970) 553.
[78] F.B. van Duijneveldt, J.G.C.M. van Duijneveldt de Rijdt, J.H. van Lenthe, Chem. Rev. 94 (1994) 1873.
[79] S.J. Ye, R.M. Moision, P.B. Armentrout, Int. J. Mass Spectrom. 240 (2005) 233.
[80] P.B. Armentrout, M.T. Rodgers, J. Phys. Chem. A 104 (2000) 2238.
[81] M.T. Rodgers, P.B. Armentrout, Mass Spectrom. Rev. 19 (2000) 215.
[82] N.N. Dookeran, T. Yalcin, A.G. Harrison, J. Mass Spectrom. 31 (1996) 500.
[85] S.J. Ye, P.B. Armentrout, J. Phys. Chem. B 112 (2008) 10303.
[86] L. Rodriguez-Santiago, M. Sodupe, J. Tortajada, J. Phys. Chem. A 105 (2001) 5340.
[87] J. Bertran, L. Rodriguez-Santiago, M. Sodupe, J. Phys. Chem. B 103 (1999) 2310.
[88] R.G. Wilson, G.R. Brewer, Ion Beams with Applications to Ion Implantation, Wiley, New York, 1973.
[89] R.M. Moision, P.B. Armentrout, in preparation.
[90] S.M. Smith, A.N. Markevitch, D.A. Romanor, X. Li, R.J. Levis, H.B. Schlegel, J. Phys. Chem. A 108 (2000) 11063.